 ICES-2017-287

In-Situ Fabricated Space Suits for Extended Exploration and Settlement

Harrison Bartlett[1], Joseph Bowser[1], Carlos Callejon Hierro[1], Sarah Garner[1],
Lawrence Guloy[1], Christina Hnatov[1], Jonathan Kalman[1], Baram Sosis[1] and David L. Akin[2]
University of Maryland, College Park, MD, 20742

Human Mars exploration will result in a demand for extravehicular activity one or two orders of magnitude beyond prior peak rates, occurring at the end of a 26-month logistics cycle. The extensive fabric "soft goods" of conventional spacesuits are subject to wear and abrasion, tend to carry dust back into the crew habitats, and replacement parts must be transported from Earth and stocked for use on need. This paper reports on the first year of an ongoing project at the University of Maryland (UMd) examining the technology of "hard suits," in combination with recent advancements in additive manufacturing, to investigate the potential for the use of hard suits in Mars exploration with on-site fabrication of replacement parts, or even entire pressure garments on need. The current focus has been on materials testing, fabrication techniques, and testing methodologies in preparation for building a hard suit joint prototype.

Nomenclature

A	=	Cross-sectional area
AX-5	=	Ames Experimental suit 5
EMU	=	Extravehicular Mobility Unit
EVA	=	Extravehicular activity
F	=	Force
FDM	=	Fused Deposition Method
ID	=	Index of Difficulty
k_1, k_2	=	Constants related to the suit arm
L	=	Initial length
PHASE	=	Printed Hard Arm Space Suit Enhancement
PLA	=	Polylactic Acid
P	=	Pressure
SLS	=	Selective Laser Sintering
SSL	=	University of Maryland Space Systems Laboratory
t	=	Thickness
δ	=	Deformation
ϵ	=	Strain
μ_T	=	Movement time
σ	=	Stress
σ_{hoop}	=	Hoop stress
σ_{axial}	=	Axial stress

[1] Undergraduate Research Assistant, Space Systems Laboratory, University of Maryland, 4436 Technology Drive, College Park, MD 20742
[2] Director, Space Systems Laboratory; Associate Professor, Department of Aerospace Engineering, University of Maryland, 4436 Technology Drive, College Park, MD 20742

I. Introduction

As advancements in technology make human exploration of Mars more feasible, it is becoming increasingly crucial that spacesuit technology is able to stand up to the extravehicular demands of such a mission. In the event of damage to spacesuits, repairs would require a stock of replacement parts or the transport of these parts from Earth. As exploration pushes further from Earth, with the potential for open-ended missions, it is especially important that astronauts develop a level of autonomy. Additive manufacturing technology (or 3D printing), in conjunction with "hard suits," presents a unique opportunity for advancement in this regard. The use of a hard suit almost entirely created using additive manufacturing techniques would allow for repairs to be made in situ and would decrease the volume required to send and/or store replacement parts and supplies.

This paper presents the first stage in design and testing of the Printed Hard Arm Spacesuit Enhancement (PHASE), a prototype hard suit arm segment made using additive manufacturing. Starting with a baseline suit kinematic configuration mirroring that of the NASA Ames AX-5 experimental spacesuit, the primary functional allocations of the suit elements were focused down to structural elements, bearings, and seals. Materials samples were tested to quantify design parameters for differing materials, fabrication methods, and even printing orientations. Bearings were fabricated with all parts or with post-fabrication insertion of steel balls, and will be tested against state-of-the-art Kaydon bearings for joint torques under load and for failure loads.

II. Joint Design

We chose to focus on the elbow joint as a proof of concept because it only has two degrees of freedom and is relatively simple to construct compared to other joints. The joint prototype is based on the design of the AX-5 elbow joint. The joint is constructed of three serially-connected truncated spherical sections. The two outer sections are spheres truncated into right triangular wedges, and the inner section is a sphere truncated into an equilateral triangular wedge. The hypotenuses of the outer wedges meet with the sides of the inner wedge. A CAD model of the prototype is shown in Figure 1, and a prototype printed in polylactic acid (PLA) is shown in Figure 2.

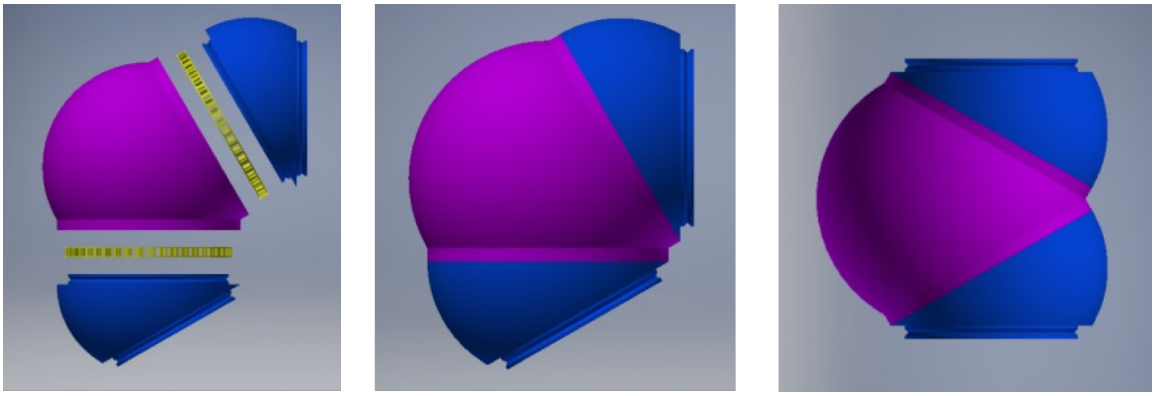

Figure 1. CAD assembly of prototype in bent and straightened orientations and with an exploded view.

Figure 2. PHASE outer and inner wedge printed using PLA.

The inner angles of the outer wedges are 30 degrees, and the inner angle of the center wedge is 60 degrees. Rotational movement is accomplished using ball bearings integrated into the ends of the wedges, shown without the surrounding wedge elements in Figure 3. The outer two wedges rotate together, and the center wedge rotates independently in the opposite direction. When the long sides of the inner and outer wedges are aligned, the sum of the inner angles create

a 120-degree bend in the joint. When the long sides of the outer wedges oppose the long side of the inner wedge, the joint is straightened. Inner bearing races are integrated into the ends of the outer wedges, and outer bearing races are integrated into the center wedge. Pressure energized lip seals, shown in Figure 4, are attached to the inner race and seal against the shelf that the outer race sits on.

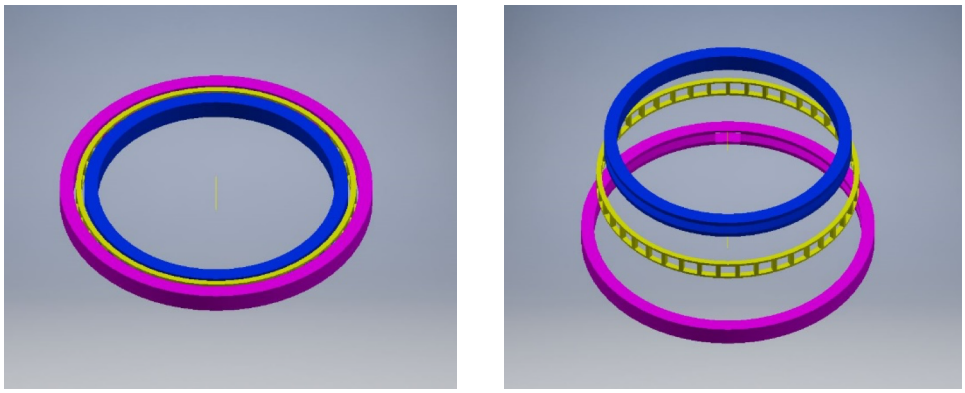

Figure 3. Bearing assembly with bearing keeper and exploded view. *The inner race (in blue) is integrated into the outer wedges, and the outer race (in violet) is integrated into the inner wedge. Balls not shown.*

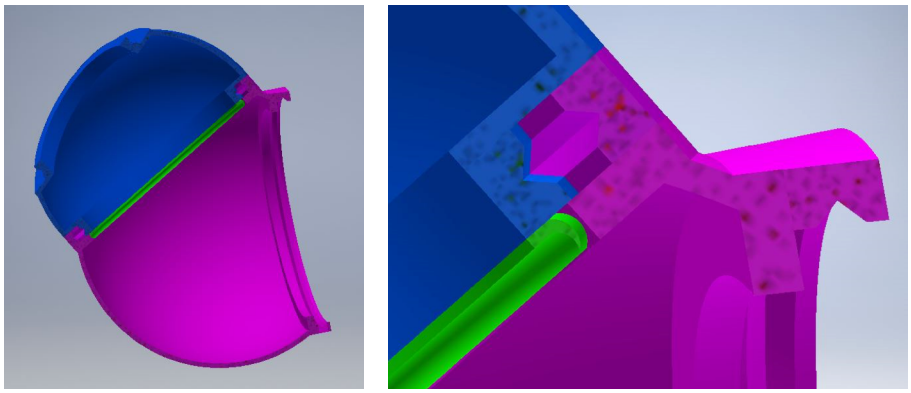

Figure 4. Cross sections of inner (blue) and outer (violet) wedge and pressure energized lip seal (green).

III. Materials Properties Testing

To ensure the structural integrity of the joint, we have begun evaluating the material properties of different additive manufacturing materials and techniques. Our primary testing methods are tension tests and hydrostatic tests; these tests have been performed to date on PLA and Stratysys' Standard Polyjet Material RGD840 Veroblue. Neither of these materials are certified to use in space, and would not be used in a final spacesuit design. We use them here only as prototyping materials to reduce costs, and as such have limited our testing to tension and hydrostatic tests. These tests were performed primarily to certify that a prototype made of these materials would be safe to test with human subjects. (Human testing is discussed below in Section V.)

A. Tension Tests

Tension tests were performed on PLA specimens using a hydraulic universal testing machine from MTS Systems Corporation to determine the effects of print orientation on tensile strength. Tests were performed on two groups of test articles: one with a cross sectional area of 0.1875 in^2 (1.201 cm^2) and the other with a cross sectional area of 0.3 in^2 (1.94 cm^2). Furthermore, each group was divided into two subgroups based on print orientation (vertical or horizontal). Specimens printed in a vertical print orientation have strands perpendicular to the long axis, while those printed in a horizontal orientation have strands parallel to the long axis. Stress-strain curves (shown in Figure 5) were calculated from the test results using Eq. (1) and (2). (σ represents stress, F represents force applied, A represents cross-sectional area, ϵ represents strain, δ represents deformation, and L represents initial length.) Average tensile

strengths are shown in Table 1; the results indicate an average tensile strength of 7150 psi for horizontally-printed specimens and 5240 psi for vertically-printed specimens.

$$\sigma = \frac{F}{A} \tag{1}$$

$$\epsilon = \frac{\delta}{L} \tag{2}$$

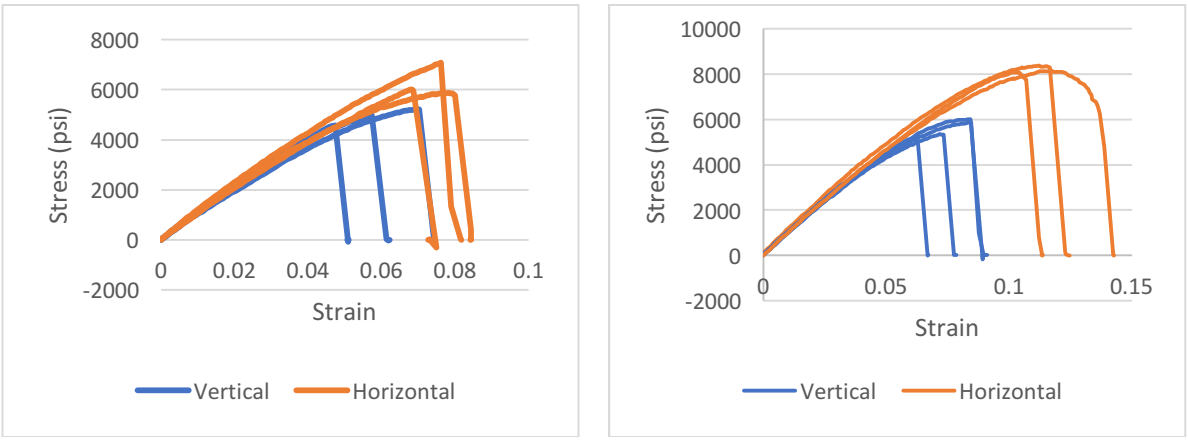

(a) **(b)**

Figure 5. Stress-strain curves of PLA specimens with cross-sectional area of (a) 0.3 in^2 (1.94 cm^2) and (b) 0.1875 in^2 (1.201 cm^2).

Table 1. Tensile test results: tensile strengths.

Area / Orientation	0.3 in^2 (1.94 cm^2)	0.1875 in^2 (1.201 cm^2)	Average
Horizontal	6174 psi	8126 psi	7150 psi
Vertical	5027 psi	5446 psi	5236 psi

In both datasets, samples printed with a horizontal orientation show signs of yielding or plastic deformation before breaking, acting as a ductile material. Samples printed with a vertical orientation show no sign of yielding or plastic deformation before breaking, acting like a brittle material. Furthermore, samples printed horizontally can withstand a higher maximum stress than those printed vertically. This is because the tensile forces acting on samples printed horizontally act along the layers, rather than perpendicular to them (as they do for samples printed vertically). The high variation in the results is due to the inconsistent quality of materials printed in PLA. In addition, as shown in Figure 6, while most of the specimens broke properly in the center, some 0.3 in^2 horizontal specimens broke on the neck of the specimen, rendering the data from those tests unusable. We believe this failure mode is caused by a combination of stress concentration at the necks of the specimens and misalignment of the strands at the necks. Although the strands in specimens printed horizontally are generally parallel to the long axis of the specimen, they become less so along the neck due to its outward curve. Thus, the strands in the neck are no longer parallel to the applied tensile forces, causing a weakness in the neck. This explains why no specimens printed vertically showed this failure mode: as there is no difference in strand orientation between the neck and the center of specimens printed vertically, there is less inherent weakness in the neck. The two failure modes are shown in Figure 6.

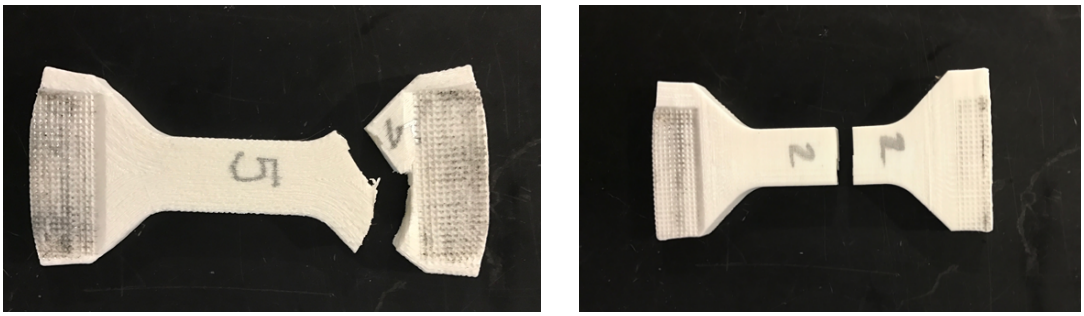

Figure 6. Two types of failure modes of PLA specimens.

In addition to performing tests on PLA, tensile tests were also performed on Veroblue specimens created via the Polyjet process. All test specimens have a cross section of 0.0491 in^2 and have a length of 1.5 in. Stress vs. strain curves (Shown in Figure 7) were produced from the tests in the same manner as the PLA tests. There were two groups of tests. The first three tests (as shown in Figure 7a) gave inconsistent strain results. Furthermore, the tensile strengths were far lower than that reported in the data published by Stratasys (around 7250-8700 psi). To increase the quality of the results, five more tests were performed (shown in Figure 7b), and results from these tests match the data published by Stratasys more closely. Specifically, the peak stresses of the first test group ranged from 5173 to 6405 psi, with an error relative to the published data of about 26-31%. Meanwhile, the peak stresses of the second group ranged from ranged from 6110 to 7450 psi with an error of about 14-16%.

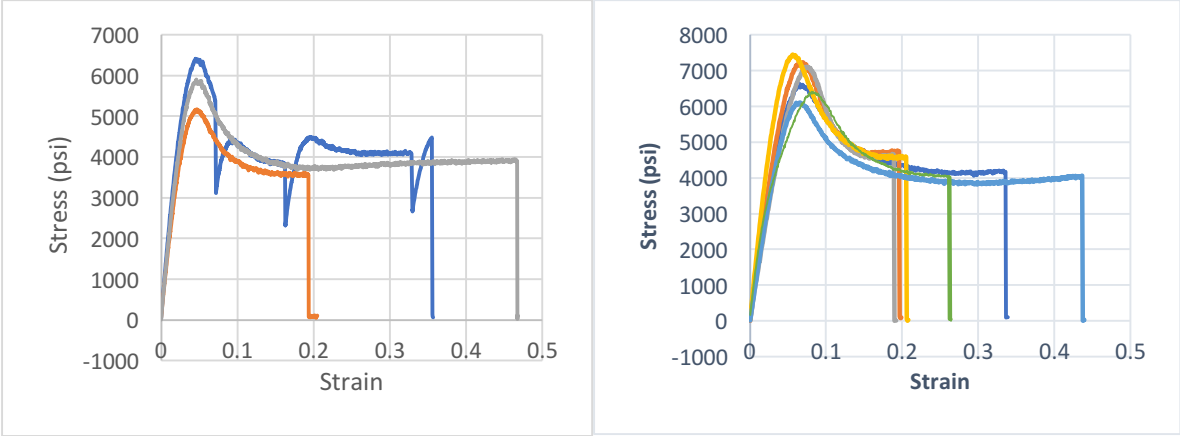

(a) **(b)**

Figure 7. Stress vs. strain curves of the two different testing groups of RGD840 Veroblue

Based on these experiments, it appears that the Veroblue's ductile behavior caused inconsistencies when these specimens failed. Figures 7a and 7b demonstrate these inconsistencies by showing multiple points of failure occurring at different strains. Despite these inconsistencies, the material has a high enough peak and yield stress that it is a viable material to use in the initial human testing discussed in Section V.

B. Hydrostatic Tests

Hydrostatic tests were also employed to assess material properties. Our prototype will have an operating pressure of 8.3 psi with a safety factor of 3 (resulting in a pressurization requirement of 25 psi); hydrostatic tests verified that our materials can hold this pressure. We printed pressure vessels (such as that shown in Figure 8) using PLA (with and without an external West Systems epoxy coating) and Veroblue to determine the pressure at which the materials leak and the pressure at which they burst. Vessels were submerged in the University of Maryland Space Systems Laboratory (SSL) neutral buoyancy tank and pressurized until they either burst or the maximum pressure of our pump was reached. Table 2 shows the results of this test, and specifies the conditions of each test specimen. (Test 2 is marked as having a "partial" epoxy coating because after the test was completed, patches of uncovered PLA were discovered near the lip of the bottle. It is unclear whether this affected test results.)

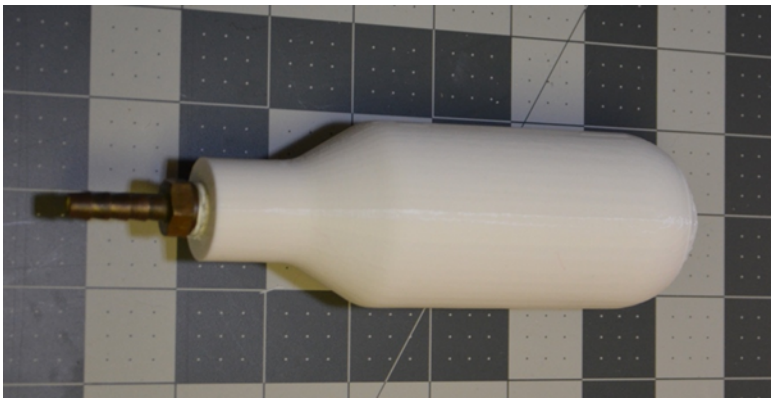

Figure 8. A pressure vessel made of PLA (uncoated).

Table 2. Hydrostatic test results and observations.

Test	Material	Wall thickness	Epoxy coating	Pressure at first leak	Source of leak	Maximum pressure	Cause of test cessation
1	PLA	1/8 in	None	<1 psi	PLA	N/A	N/A
2	PLA	1/8 in	Partial	90 psi	Inconclusive	100 psi	Hose detached from tap
3	PLA	1/16 in	Full	55 psi	Improperly sealed tap	80 psi	To replace tap
4	PLA	1/16 in	Full	90 psi	Tap	140 psi	Maximum pump pressure
5	Veroblue	1/16 in	None	N/A	N/A	80 psi	Surpassed required safety limit
6	Veroblue	1/16 in	None	<1 psi	Crack in the specimen	N/A	N/A
7	Veroblue	1/16 in	None	N/A	N/A	80 psi	Surpassed required safety limit
8	Veroblue	1/16 in	None	N/A	N/A	80 psi	Surpassed required safety limit

As shown in Table 2, coating the pressure vessels in epoxy significantly impacts the pressure the vessel can hold. Tests 2-4 demonstrate that when an epoxy coating is used, leaks were observed (if at all) at pressures of 55 psi and up. Meanwhile, with no coating, leaks were observed at less than 1 psi. Furthermore, we did not observe any violent failure modes: tests 2 and 3 were terminated because of problems with the tap used to secure the pump to the pressure vessel, whereas test 4 was terminated because the maximum pressure of our pump was reached. In no test did the pressure vessel itself burst. Based on these observations, we have concluded that PLA pressure vessels coated with epoxy can withstand a pressure differential of at least 25 psi. Veroblue, on the other hand, can hold pressure without a coating, which makes it a valid material for pressurized parts. The only failure in testing Veroblue occurred due to a crack in the specimen, believed to be due to damage to the specimen before testing. The Veroblue specimens in tests 5, 7, and 8 did not show any signs of failure before exceeding the required safety limit of 80 psi. Based on these observations, Veroblue can withstand a pressure differential of 25 psi without the aid of any coating.

To better quantify the material strength under a hydrostatic test, we converted the pressure data into stress data using Eq. (3) and (4). (σ_{hoop} and σ_{axial} represent hoop and axial stress, respectively; P represents pressure inside the test specimen; r represents the radius of the specimen; and t represents the thickness of the specimen.) The corresponding hoop and axial stresses are displayed in Table 3. Converting the data to hoop and axial stresses allows us to compare the tensile strengths of the materials used in hydrostatic testing to other published data, and to our own experimental results. Experiments reported in Section IIIA above found an average tensile strength for PLA of 7150 psi for horizontally-printed specimens and 5240 psi for vertically-printed specimens, both far higher than the maximum hoop and axial stresses exerted in the hydrostatic tests. This is consistent with the results of the

hydrostatic tests: while several tests failed due to issues with the tap or pump, none of the PLA test cylinders shattered or fractured. Comparable results were found during hydrostatic tests of Veroblue samples. Stratasys reports a tensile strength for the material of 7250-8700 psi[1], significantly higher than the maximum stresses exerted during hydrostatic testing. This explains why no Veroblue samples failed during testing. (The one cracked sample likely cracked before testing began, as explained above.)

$$\sigma_{hoop} = \frac{Pr}{t} \tag{3}$$

$$\sigma_{axial} = \frac{Pr}{2t} \tag{4}$$

Table 3. Hydrostatic test results by hoop and axial stresses

Test	Material	Hoop stress at first leak	Axial stress At first leak	Maximum hoop stress reached	Maximum axial stress reached
1	PLA	<1 psi	<1	N/A	N/A
2	PLA	720 psi	360 psi	800 psi	400 psi
3	PLA	880 psi	440 psi	1280 psi	640 psi
4	PLA	1440 psi	720 psi	2240 psi	1120 psi
5	Veroblue	N/A	N/A	800 psi	400 psi
6	Veroblue	N/A	N/A	800 psi	400 psi
7	Veroblue	<1 psi	<1 psi	N/A	N/A
8	Veroblue	N/A	N/A	800 psi	400 psi

C. Discussion of Results

Based on these results, we have determined that PLA, due to its low print resolution and inability to hold pressure without a coating, is largely unsuitable for use in our final prototype. However, it can be used as a cheap substitute for more expensive materials when prototyping the static elements of the joint (such as the wedge elements) if pressurization is not needed. As such, future unpressurized tests of the prototype will employ wedge elements made in PLA. Veroblue, on the other hand, can likely be used to construct effective seals due to its high print resolution and ability to hold pressure. (Initial tests of a seal prototype made with Veroblue are discussed in Section IV.) While its inconsistent material properties make it a weak candidate for use in a final prototype, it can be used as an analogue for more expensive materials during design and testing. Future work will involve tests of parts printed in Duraform GF to replace those made in PLA and Veroblue (as discussed in Section V).

IV. Component Assembly Design and Testing

Understanding the material properties of common additive manufacturing materials would not be meaningful if creating spacesuit components using them were infeasible. To this end, the focus in this area has been on the fabrication of bearing assemblies and lip seals using a maximal amount of 3D printing.

A. Bearing Development

Past work[2] started with the fabrication and testing of a 6in bearing, fabricated complete in a single build process using fused deposition method (FDM) on a Stratasys UPrint-30 system. This bearing was the proof-of-concept for a fully 3D printed bearing, but relied on the availability of a relatively high-precision machine with dissolvable support material. Tests in the as-fabricated condition were favorable, but the bearing worked more smoothly and with less friction when the 3D printed balls were replaced with 0.25 in precision stainless steel balls made for use in bearings.

The next stage of component fabrication tests focused on both isolated bearings and suit arm wedge elements connected by ball bearings, as shown in Figure 4. A port for adding or removing balls is designed into the outer race, and the inner and outer races are held aligned in plane with the bearing keeper structure concentrically placed between

them. Balls are introduced into the bearing at widely distributed locations to force concentricity and "lock" the pieces together, then the components are rotated until all of the locations in the bearing keeper are filled with balls. A small cover which fits into the ball port is used to capture the balls in the bearing; the cover has a matching inside profile that fills out the outer race when locked in place. The initial test pieces were fabricated on consumer-grade FDM, specifically several Rostock v2 machines, using PLA filament. These test pieces were too low in fabrication accuracy to produce acceptable bearing races, but proved out the basic design and dimensions of the printed bearing structures.

As the next step, a 4.5 in test bearing was fabricated using the same design approach on a Polyjet Objet30 Pro printer in Veroblue material. The choice of size was to match a Kaydon KA45-XP bearing, the type used in the AX-5 wrist roll joint. The two bearings are shown side-by-side in Figure 9. The Kaydon bearing uses 3/32 in balls, and has a 0.25x0.25 in cross section. The 3D printed bearing was sized for 0.25 in balls, resulting in a cross-section of 0.325 in deep by 0.625 in radially. The 3D printed bearing was designed with different dimensions than the Kaydon bearing to account for the lower resolution of the 3D printers. This lower resolution cannot achieve the tolerances necessary to fabricate an exact replica of the Kaydon bearing. The inner and outer races and bearing keeper were printed simultaneously in a concentric configuration, and populated with 30 0.25 in steel balls. The printed bearing is shown disassembled in Figure 10. Both the Kaydon and Veroblue printed bearings were tested for required rotation torque; both were too low in rotational friction to be measured by the available test set-up, which has a minimum resolution of 100 mNm.

Figure 9. Kaydon metal and Polyjet-printed Veroblue plastic bearings

Figure 10. Polyjet-printed Veroblue plastic bearing with steel balls disassembled

This process to date has demonstrated that accurate additive manufacturing techniques can produce bearings which rival commercially-available conventional bearings for joint torque. While the Veroblue material is not suitable for a pressurized suit due to low tensile modulus and high elongation at tensile failure (typically 20%), the availability of on-campus Polyjet printers allowed iteration and verification of designs at a reasonable cost to the program. Future steps in this area include investigating the use of smaller balls and races to reduce the cross-sectional areas of 3D printed bearings, using designs verified in Veroblue to order bearing components in Duraform GF ("Glass Filled") via selective laser sintering (SLS) from service bureaus, and doing axial, radial, and transverse torque loads testing of the resultant test articles to find the strength and durability of parts created using SLS. The finer surface finish produced via Polyjet or SLS processes will also be used to evaluate 3D printed seal concepts.

B. Lip Seal Development

The PHASE Mk. 1 design calls for a single lip seal for each bearing to retain pressure within the suit. To further our goal of maximizing the potential for in-situ fabrication of our prototype, we fabricated these seals on the Polyjet machine using Stratasys' TangoBlackPlus FLX rubber-like material.

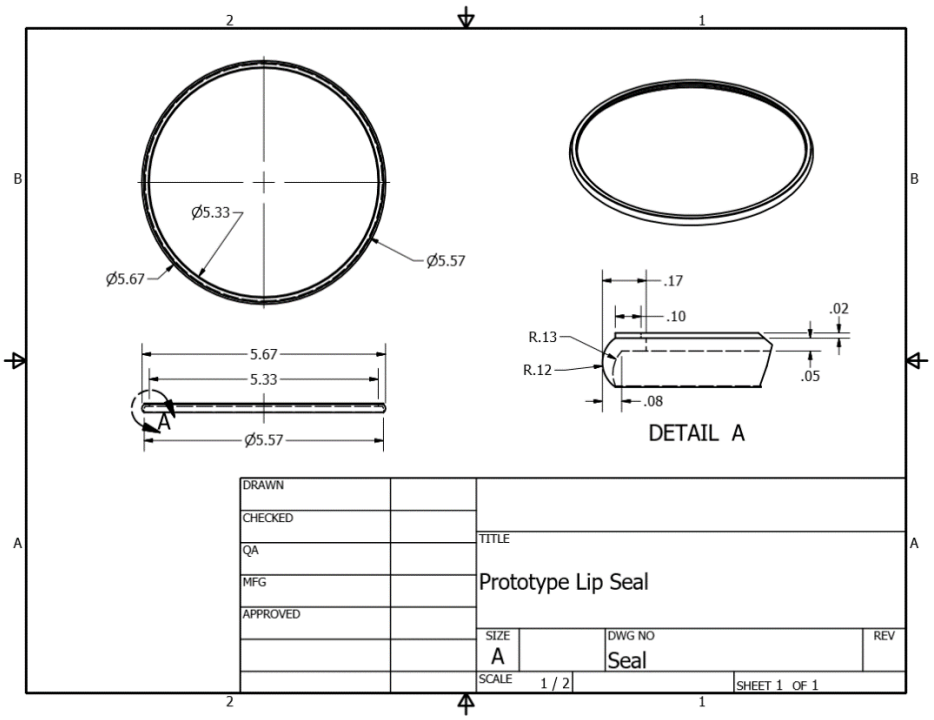

Figure 11. Dimensioned drawing of lip seal that is integrated into the inner bearing race of the Mk. 1 prototype.

In order to evaluate the integrity of this seal, we designed a customized bearing that takes advantage of the printer's ability to print in multiple materials to print an integrated seal. This bearing, shown in Figure 12, was designed for testing at differential pressure in the SSL glovebox.

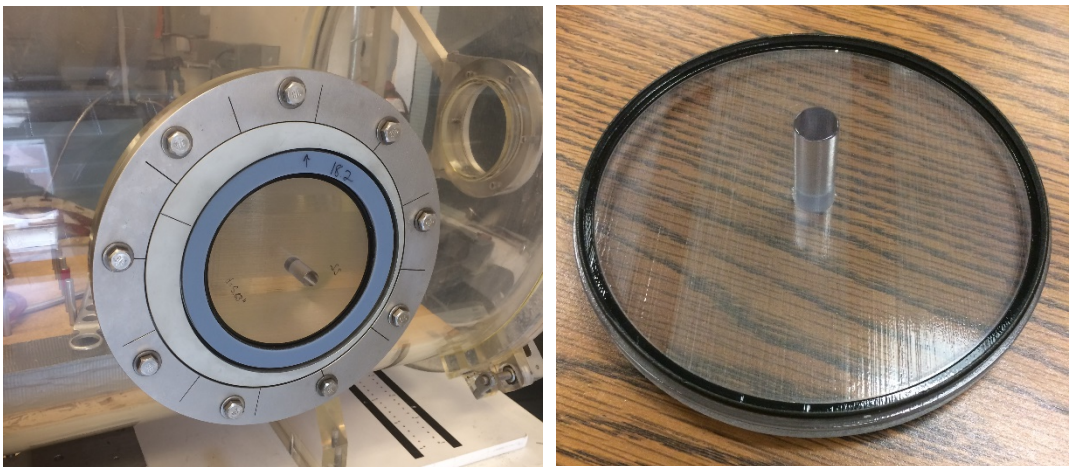

Figure 12. The seal evaluation bearing. *The blue outer race integrates into the SSL glovebox, allowing the transparent inner race to rotate under differential pressure. The prototype seal is visible in black.*

Initial testing demonstrated that the 3D printed seal was not adequate to retain a pressure differential of 4.3 psi. As shown below in Figure 13, the pressure differential caused the seal to fail by being "sucked" into the bearing at approximately 2.5 psi. We intend to further investigate the properties of 3D printed rubber-like materials, as we believe this failure was due to inadequate seal design and material. Increasing seal thickness can improve the rigidity of the seal. We will be able to vary the hardness of rubber-like material by experimenting with multi-material prints using different combinations of rigid and flexible material. Pending further evaluation, we expect 3D printed rubber-like

materials will be used for pressure retention in future design iterations. However, if additional tests are unsuccessful, the PHASE Mk. 1 and future design iterations can be simply modified to utilize traditionally fabricated lip seals.

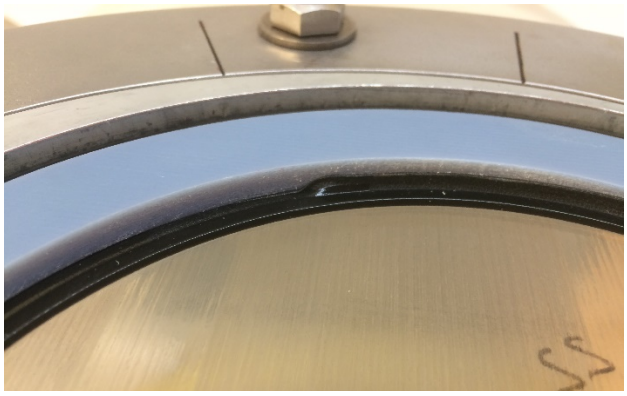

Figure 13. Result of initial seal testing in the glovebox. *A portion of the lip seal was pulled into the bearing due to the pressure differential. This failure prevented the bearing from holding pressure and being able to rotate.*

V. Directions for Future Research

Current plans for future work include finalizing our prototype using space-grade materials and refining our seal design, as well as human testing of the final prototype to validate usability. Further design iterations based on the results of the testing data will lead to the development of the PHASE Mk. 2 over the coming 18-24 months.

A. Additive Manufacturing

Currently, much of our prototyping has been completed in PLA on fused-deposition modeling machines. This was a logical choice, as it is inexpensive and readily available with the UMd Space Systems Laboratory. PLA is not rated to fly in space, however, and presents several design challenges. Due to variance in tolerances between FDM, Polyjet, and SLS printing processes, we decided that PLA is not an adequate prototyping material for parts with tight tolerances, such as bearings. Due to the closer similarities between materials manufactured using Polyjet and SLS processes compared to FDM process, we decided to eliminate PLA as a prototyping material, proceeding with prototyping in Veroblue and leaving Veroblue, Windform XT, and Duraform GF as potential final material choices.

Veroblue was chosen as the main prototyping material because it is a relatively cheap analog for Duraform GF and Windform XT, and will reduce the cost of validating our designs and performing basic tests. Initial testing currently suggests that printing with Veroblue is not a viable means of producing our final prototype, due to highly inconsistent material properties and the tendency of these polymers to degrade when exposed to high-intensity ultraviolet light. However, its low cost, high precision fabrication, and ability to retain pressure make it a suitable prototyping material for the more expensive Windform XT and Duraform GF.

Ultimately, a suit developed using our design would be printed in Windform XT, a space-rated plastic printed using SLS machines. Windform XT is prohibitively expensive, however, likely eliminating its use in our prototyping process. As an alternative, we plan to explore the properties of Duraform GF, a glass-infused nylon material which can also be printed using SLS processes. We believe that Duraform GF will serve as an appropriate analog for Windform XT, and we intend to test a Duraform GF prototype in vacuum to determine outgassing characteristics.

B. Seal Design

We also plan to improve the design of our seals to increase redundancy and reduce friction. Currently, pressure retention within the wedge elements is accomplished by a single lip seal, installed on a shelf inside of the wedge elements. Traditionally, spacesuit bearings are sealed using Y-separator seals or multiple redundant lip seals; the second iteration of our design will investigate more advanced seal designs than the single lip seal discussed here. Our current prototype also seals directly against the 3D printed surfaces of the wedge elements. Such a design may not be sufficient to fully seal our prototypes, and may result in high friction between the seal and the wedge element. In preparing for our next design iteration, we will analyze this friction and, if necessary, will install small metal strips to create a smoother sealing surface. While this would somewhat reduce the potential for in-situ fabrication, these parts are low mass and volume, and can be easily transported and stored in large quantities.

C. Testing

To qualify and improve our prototype, we will conduct tests of its parts in isolation and compare its performance to published data. We will compare our printed bearings to commercially available, traditionally fabricated bearings; our goal is for the additive manufacturing process to increase the torque required for motion by no more than 50%. The prototype will also be qualified through a series of tests in the SSL glove box, where its range of motion will be measured and human trials will be completed. We expect to achieve a range of motion of 120 degrees during this testing.

Our human trials will give us the most complete description of the comfort and usability of our prototype. We will use Fitts' Law protocols to quatitatively compare the difficulty of movement of a Shuttle-era Extravehicular Mobility Unit (EMU) arm currently in the SSL's possession to our prototype arm. Fitts' Law was first described in 1954, and has become a standard in physiological research owing to its robust empirical regularity. The law states that the time required to touch a target is a function of the ratio between the starting distance from the target and the size of the target.[3] Fitts' Reciprocal Tapping Test, based on Fitts' Law, is often used to estimate the difficulty of a motion. Our version of this test uses two metal plates and a metal-tipped stylus which the subject is instructed to reciprocally tap on each plate as fast as possible.[4] By instructing the test subjects to minimize their errors while working against a time limit, subjects will naturally adjust the speed of their movement, so that more difficult movements result in fewer total taps than simpler ones in a set time interval.[4] Data collected from the tapping test is then analyzed using Eq. 5:

$$\mu_T = k_1 + k_2 \times ID \tag{5}$$

μ_T is movement time from one target to the next, k_1 and k_2 are constants related to adjusted variables, and ID is the Index of Difficulty, which is determined by the dimensions of the testing device.[3] Our test will evaluate four different indices of difficulty, accomplished by varying both the arclength between targets and the size of the targets themselves. The design of our Fitts' board is shown in Figure 14, with the different arc lengths we will analyze noted. These paths were selected to analyze performance across varying ranges of motion, and at different starting angles of the elbow.

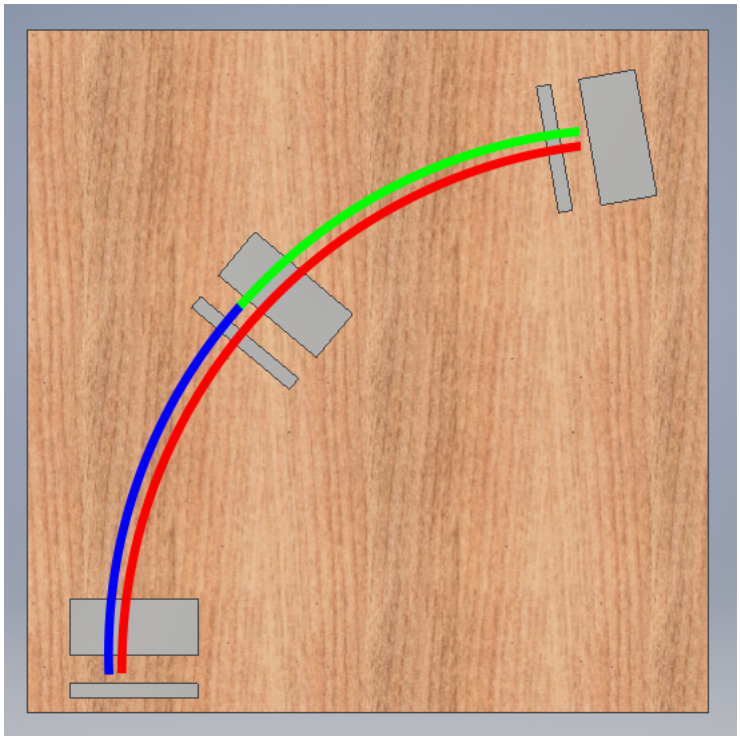

Figure 14. Diagram of the Fitts' board setup, with evaluated ranges of motion. *Red corresponds to a movement from 10° to 90°, green from 10° to 50°, and blue from 50° to 90°. These ranges of motion will be evaluated between both the small and large targets.*

Since all four indices of difficulty will be completed while wearing both the EMU and PHASE Mk. 1, ID can be treated as a constant for any given set of test parameters. This means any change in μ_T is due only to k_1 and k_2, which

are directly related to our independent variable, the suit arm. Thus, we can derive the difference in movement difficulty between the two test suit arms directly from the change in μ_T. Research participants will also complete a comfort survey regarding both our prototype and the EMU suit arm. We expect to conduct tests with at least 15 individuals. The criteria we will use to select subjects are that they must have full use of their right arm, and that their right arm must fit in the SSL's EMU arm. Although these criteria would not be necessary if we were only testing on a 3D printed arm, as we could easily print parts of different sizes, the need to test on the SSL's single EMU arm necessitates these restrictions.

We will assess the comfort of our joint using a simple questionnaire, modeled after that used in Ref. 5. After our research participants complete the Fitts' Reciprocal Tapping Test, they will evaluate their level of comfort on the questionnaire via a Likert scale, where participants specify their level of agreement or disagreement with statements about the suit's comfort.[6] We will further ask the participants to identify any uncomfortable points of contact between their arm and the suit. Questionnaire results will be collected both from trials using our suit arm and from those using the EMU, allowing us to compare the comfort of the two suits. Subjective evaluations of arm operations will be collected via the use of a modified Cooper-Harper rating and the NASA Task Load Index.

At the time of our presentation, we anticipate having completed our testing of bearings, as well as our range of motion and human trials in the SSL glove box. We intend to replicate our current PLA prototypes in Duraform GF pending the material's successful completion of hydrostatic testing, which we also anticipate will be complete at the time of our presentation. Using the data gathered from these tests, we will fine-tune our wedge element and seal design and conduct a second round of testing over the next 18-24 months, resulting in a second prototype, the PHASE Mk. 2.

VI. Conclusion

The results of these tests demonstrate that production of spacesuit components using additive manufacturing may be attainable in the near future. Although our research was conducted using low-cost materials and processes, we demonstrated the basic feasibility of using 3D printed materials as pressure vessels. Test cylinders made with PLA, while inexpensive, are capable of withstanding pressures well over 25 psi (providing a safety factor of 3) when coated with epoxy; vessels made with Veroblue can hold this pressure without a coating. Future work will attempt to replicate these tests using higher quality materials.

Initial tests also indicate that while the development of sealed rotary bearings using 3D printed materials may be feasible, significant challenges remain. Current prototypes are unable to hold the required pressure differential; future tests involving refined seal designs and higher-quality materials are needed to further explore the possibility of 3D printing sealed rotary bearings.

Improvements in the field of additive manufacturing can help enable new long duration space missions. One reason the AX-5 was never flown is its high stowage volume. Additive manufacturing can help mitigate this problem, as the volume taken up by the bulk material necessary to print a spacesuit is much less than that taken up by the completed suit. Additionally, if an additively manufactured hard suit is damaged on long duration missions, it can be repaired relatively easily by printing new components, rather than requiring stockpiles of backup suit parts. These advantages can enhance the feasibility of currently-planned long duration missions, and open up new mission profiles to planners.

Acknowledgments

We would like to acknowledge the University of Maryland Space Systems Laboratory for the support and resources provided by the lab, as well as Lemuel Carpenter and Dr. Andrew Becnel for their invaluable advice and assistance with testing. Additionally, we would like to thank NASA's eXploration Systems and Habitation (X-Hab) 2017 Academic Innovation Challenge for funding this research, especially Tracie Prater, technical monitor. Finally, we would like to thank the University of Maryland's Gemstone Honors Program for providing the opportunity to engage in an extensive multidisciplinary research project as undergraduate students.

References

[1]"PolyJet™ Materials Data Sheet", Stratasys.com, 2014. [Online]. Available: http://www.stratasys.com/materials/polyjet/~/media/29592222B80C489BAC28803DB08C10E5.ashx. [Accessed: 10- May- 2017].

[2]D. L. Akin and K. Davis, "Hard Suits/Soft Suits: Revisiting Technologies and Applications for a New Space Era" ICES-2015-268, 45th International Conference on Environmental Systems, Bellevue, Washington, 12-16 July 2015

[3]Y. Guiard and H. B. Olafsdottir, "On the Measurement of Movement Difficulty in the Standard Approach to Fitts' Law," PLoS, vol. 6, no. 10, pp. e24389, Oct. 2011. doi: 10.1371/journal.pone.0024389, [Online]. Available: http://journals.plos.org/plosone/article?id=10.1371/journal.pone.0024389

[4]P. M. Fitts, "The Information Capacity of the Human Motor System in Controlling the Amplitude of Movement," *J. of Experimental Psychology*, vol. 47, no. 6, pp. 381-391, Jun. 1954.

[5]B. Feng et al. "Are 'Smart Pressure Monitored Suits' 'Smarter' than Conventional Garments in Clinical Applications?" *Hong Kong J. of Occupational Therapy*, vol. 23, no. 2, pp. 82-88, Dec. 2013.

[6]R. Likert, "A technique for the measurement of attitudes," Ph.D. dissertation, Dept. Psychology, New York Univ., Ney York, 1932.